J Appl Electrochem (2010) 40:1019–1028
DOI 10.1007/s10800-009-0051-8

ORIGINAL PAPER

The influence of electrolyte composition on electrochemical ferrate(VI) synthesis. Part I: anodic dissolution kinetics of pure iron

Zuzana Mácová · Karel Bouzek · Virender K. Sharma

Received: 9 May 2009 / Accepted: 1 December 2009 / Published online: 20 December 2009

Abstract The influence of anolyte composition and temperature on the anode dissolution kinetics of pure iron and subsequent ferrate(VI) production was studied by means of potentiodynamic voltammetry and electrochemical impedance spectroscopy. The results obtained were verified by batch electrolyses. Pure NaOH, KOH, and mixtures thereof were used as an anolyte. The motivation for this study is to understand in more detail the electrolysis process at which ferrate(VI) is electrochemically produced in situ in the solid form which is more suitable for practical utilization. A significant impact of the anolyte composition on the system behavior was indicated. It is related to the solubility of the anode dissolution products in the anolyte. It was concluded that the fast reaction kinetics in the transpassive potential region is connected with a deterioration of the ferrate(VI) synthesis efficiency. This is explained by the kinetic enhancement corresponding to the intensification of oxygen evolution as a parasitic reaction.

Keywords Ferrate(VI) formation · Iron dissolution · Electrolyte composition · Electrochemical impedance spectroscopy · Cyclic voltammetry

Z. Mácová · K. Bouzek (✉)
Department of Inorganic Technology, Institute of Chemical Technology Prague, Technická 5, 16628 Prague 6, Czech Republic
e-mail: bouzekk@vscht.cz

V. K. Sharma
Chemistry Department, Florida Institute of Technology, 150 West University Boulevard, Melbourne, FL 32901, USA

List of symbols

j_T	Experimentally determined current density (mA cm^{-2})
j_K	Kinetics of charge transfer controlled current density (mA cm^{-2})
j_D	Mass transfer controlled current density (mA cm^{-2})
n	Number of electrons exchanged
F	Faraday constant (96 485 C mol^{-1})
r	Electrode radius (cm)
D_A	Diffusion coefficient of electroactive specie A (cm^2 s^{-1})
c_A^b	Concentration of the electroactive specie A in the bulk of the solution (mol cm^{-3})
υ	Kinematic viscosity of the solution (cm^2 s^{-1})
ω	Angular rotation rate of the electrode (rad)

1 Introduction

Since the first half of the eighteenth century, it has been known that iron can be oxidized up to the oxidation state +VI [1]. With few exceptions no systematic attention was, however, paid to this class of compounds until the last two decades. This was due to its complicated synthesis and low stability. The recently arising interest is motivated mainly by the increasing importance of potential ferrate(VI) application fields. This especially concerns water treatment technology. The advantage of ferrate(VI) utilization in this particular technology is mainly related to its strong oxidation power and excellent coagulation properties of $Fe(OH)_3$ as ferrate(VI) reduction product [2].

Three basic methods of ferrate(VI) preparation, dry, wet, and electrochemical, have been reported in the literature. The dry method consists in oxidation of a Fe(III) salt in a molten mixture of nitrate salts with potassium hydroxide

[3]. The wet method comprises oxidation of Fe(III) by hypochlorite in a concentrated KOH solution. Today, it is the most commonly employed method of ferrate(VI) preparation [4, 5].The last method is the anodic oxidation of iron. This was first reported by Poggendorf [6]. Even though this method provides a product of high purity and the procedure is easy to operate, it still remains relatively unexplored. This is probably due firstly to the high production costs, resulting from a significant demand for electrical energy. The second reason is that so far the product prepared in this way is mainly available in the form of a strongly alkaline solution. This is because the majority of authors identified concentrated NaOH solution as the most suitable environment for electrochemical ferrate(VI) synthesis [7–13]. Unfortunately, sodium salt of ferrate(VI) is well soluble. Thus, in the majority of cases it is unsuitable for direct application. Moreover, in this form it is stable for only a limited period of time (units of hours). An important prerequisite for the broader application of ferrate(VI) electrochemical synthesis is, therefore, to develop a reliable method of producing it efficiently in a solid, and thus stable, form.

The application of KOH solution as an anolyte was considered to be a promising approach to accomplish this task [14]. Since potassium ferrate(VI) was shown to precipitate at concentrations significantly lower than sodium salt [15], it was assumed that ferrate(VI) may precipitate in the solid form directly in the anode compartment. However, compared to the NaOH solution, when using KOH solution as an anolyte a significant drop in process efficiency was observed in the temperature range studied [14]. This was explained in terms of precipitation of potassium ferrate(VI) or its intermediates directly at the anode surface. It was thus inhibited from further ferrate(VI) production. This problem was overcome by Lapicque and Valentin [16]. They used a mixture of NaOH and KOH as the anolyte. Using a solution containing an appropriate ratio of sodium and potassium ions allowed them to take advantage of the low solubility of ferrate(VI) in a K^+ ion environment while maintaining high efficiency of the synthesis process. Thus, for the first time solid ferrate(VI) was prepared in the anolyte phase directly during its electrochemical production.

He et al. [17] reported the electrochemical synthesis of solid K_2FeO_4 directly from a pure KOH solution. The anode surface inhibition was suppressed here by the elevated electrolysis temperature of 65 °C. Since ferrate(VI) is produced in a solid form, its decomposition, which accelerated in the homogeneous phase due to the elevated temperature, does not represent a serious problem in this case.

Even though highly interesting results have been obtained by means of anolyte solutions containing K^+ ion, no deeper analysis of its influence on anodic dissolution and the subsequent ferrate(VI) formation process has been reported in the literature so far. It is the aim of this study to contribute to an understanding of this phenomenon. Five solutions of constant OH^- concentration of 14 M and of different Na^+ and K^+ ion ratio were used in this study. Pure iron was employed as the anode. Potentiodynamic voltammetry (PV) and electrochemical impedance spectroscopy (EIS) were applied to study the process in the first instance. The postulated theory of the influence of K^+ ion on the dissolution of the pure iron anode was subsequently verified by batch electrolysis.

2 Experimental

2.1 Chemicals

NaOH and KOH of p.a. grade (Penta, Czech Republic) were used. In all cases the OH^- concentration of the prepared electrolytes was 14 M. The solution composition varied with respect to the ratio of the Na^+/K^+ ion content. Besides pure NaOH and KOH solutions, mixtures of the Na^+/K^+ molar ratio of 1:1, 1:3, and 3:1 were also investigated.

The working electrode was made of pure iron (99.95 wt% Fe) containing the following main impurities (wt%): C—0.005, Ni—0.0048, and Mn—0.0003.

2.2 Apparatus and procedures

All cyclic voltammetric (CV) and EIS experiments were carried out in a classical three-electrode arrangement. The electrolyte temperature was thermostatically controlled. The geometric area of the working electrode comprised 0.28 cm^2 in the case of CV experiments and 0.25 cm^2 in the case of EIS experiments. The inactive electrode surface was insulated by Teflon. The electrode pre-treatment included polishing of the iron surface with emery paper P4000 (Buehler), followed by subsequent washing with distilled water and ethanol. A smooth platinum sheet with an active area of 0.84 cm^2 served as an auxiliary electrode. A HgO/Hg electrode in 14-M NaOH solution connected with the experimental cell using a Haber–Luggin capillary was used as the reference. All potentials given in the text refer to this electrode.

The potentiodynamic measurements were carried out using a PINE potentiostat AFCBP 1 (USA) controlled by a personal computer with PineChem 2.7.5 software. A MSRX Rotator by PINE Instruments was used for the experiments on the rotating ring-disk electrode (RRDE). The ring electrode was made of platinum. Its potential was held at a value corresponding to the FeO_4^{2-} reduction, i.e., at 300 mV [18, 19].

A Solartron SI 1287 electrochemical interface and a 1250 frequency response analyser (Schlumberger, UK) controlled by personal computer with ZPlot/ZView software (Scribner Associates, USA) were employed to accomplish the EIS experiments.

Prior to each experiment the electrode was polarized cathodically at approximately 20 mA cm^{-2} for 5 min to ensure a reproducible state of the electrode surface. In the case of the CV experiments, the recording of the polarization curve followed immediately after prepolarization. In the case of EIS, the electrode potential was held at a value selected for the particular experiment for 10 min to ensure steady state conditions. After that, an impedance spectrum in the frequency range of 65 kHz to 10 mHz was recorded. An ac signal amplitude of 10 mV was used. The experiments were performed under nitrogen atmosphere.

The batch electrolysis experiments were carried out in galvanostatic mode in a batch electrolytic cell with anode and cathode compartments separated by a PVC diaphragm. A detailed cell description can be found elsewhere [10]. The active anode surface was 43.1 cm^2. The anolyte volume comprised 69 cm^3. Prior to the experiment the anode was polarized cathodically at 20 mA cm^{-2} for 30 min.

The standard chromite method [5] was used to determine the ferrate(VI) content in the anolyte solution after 180 min of electrolysis. The total Fe content was determined by means of atomic absorption spectrophotometry. For this purpose a VARIAN SPECTRAA 30 equipped with a graphite furnace GTA 96 (Varian Inc., USA) and with a PHOTRON hollow cathode discharge lamp (Photron Pty Ltd.; Australia) with an emission spectrum suitable for Fe determination were used.

3 Results and discussion

3.1 Voltammetric analysis

A comparison of the potentiodynamic curves of the pure iron electrode in concentrated NaOH and KOH solution is shown in Fig. 1.

Both curves show typical behavior of the iron in a highly concentrated hydroxide solution [18, 20–22]. They are characterized by three anodic peaks, AI to AIII, appearing in the potential region of active anode dissolution. They have been previously [19] assigned to the oxidation of metallic Fe to Fe(II) (peak AI, Eq. 1), Fe(II) to Fe(III) (peak AII, Eqs. 2A–2C) and to the restructuring of the anode surface layer (peak AIII).

$$Fe + 2OH^- \rightarrow Fe(OH)_2 + 2e^- \quad (1)$$

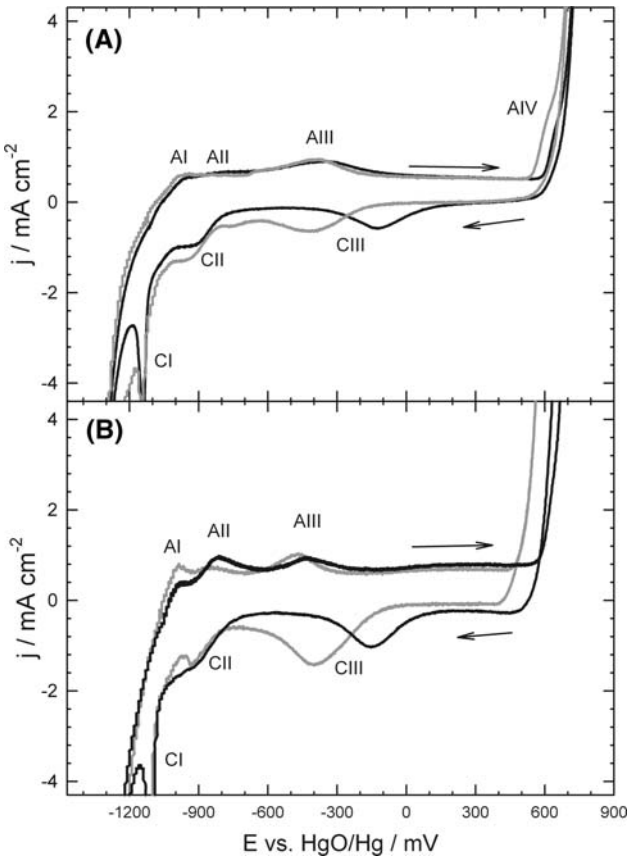

Fig. 1 Comparison of the CV curves of the Fe electrode obtained in 14-M NaOH (*black line*) and 14-M KOH (*gray line*), temperature 20 °C (**a**) and 60 °C (**b**), potential scan rate of 5 mV s^{-1}. The *arrows* indicate the potential scan direction

$$Fe(OH)_2 + OH^- \rightarrow Fe(OH)_3 + e^- \quad (2A)$$

$$Fe(OH)_2 + OH^- \rightarrow FeOOH + H_2O + e^- \quad (2B)$$

$$2Fe(OH)_2 + 2OH^- \rightarrow Fe_2O_3 + 3H_2O + 2e^- \quad (2C)$$

An alternative explanation is the formation of nonstoichiometric magnetite at the electrode potential corresponding to peak AII (Eq. 3) and its subsequent oxidation to Fe(III) (Eq. 4).

$$3Fe(OH)_2 + 2OH^- \rightarrow Fe_3O_4 + 4H_2O + 2e^- \quad (3)$$

$$2Fe_3O_4 + 2OH^- \rightarrow 3Fe_2O_3 + H_2O + 2e^- \quad (4)$$

The solid oxides and hydroxides formed on the surface of the anode are subject to chemical dissolution by interaction with the hydroxyl ion (see e.g., Eqs. 5A–5C).

$$Fe(OH)_2 + 2OH^- \rightarrow FeO_2^{2-} + 2H_2O \quad (5A)$$

$$Fe_3O_4 + 4OH^- \rightarrow 3FeO_2^- + 2H_2O + e^- \quad (5B)$$

$$Fe_2O_3 + 2OH^- \rightarrow 2FeO_2^- + H_2O \quad (5C)$$

Currently there is no information on the portion of the solid phase being dissolved during the oxo-hydroxidic film formation. It is strongly influenced mainly by the potential scan rate and by the nature, concentration, and temperature of the electrolyte [23].

After the active dissolution region, a broad passivity plateau follows and subsequently an intensive oxygen evolution reaction overlapping the transpassive iron dissolution, including ferrate(VI) formation, takes place. A current density shoulder AIV in the potential region of the commencement of oxygen evolution indicates the later process. This appears at an anode potential of 600 mV. This value is in agreement with the range of 500–700 mV reported in the literature [18–21]. At the temperature of 60 °C peak AIV is not shown on the figure because it is out of the current density axis scaling.

In the cathodic direction a current peak of ferrate(VI) reduction occurs at potentials of −70 to −300 mV (peak CIII), again depending on the electrolyte and temperature used [18–22, 24]. Peak CIII is followed by the series of current peaks belonging to the reduction of the surface layer back from Fe(III) to Fe(II) (peak CII) and subsequently to Fe(0) (peak CI).

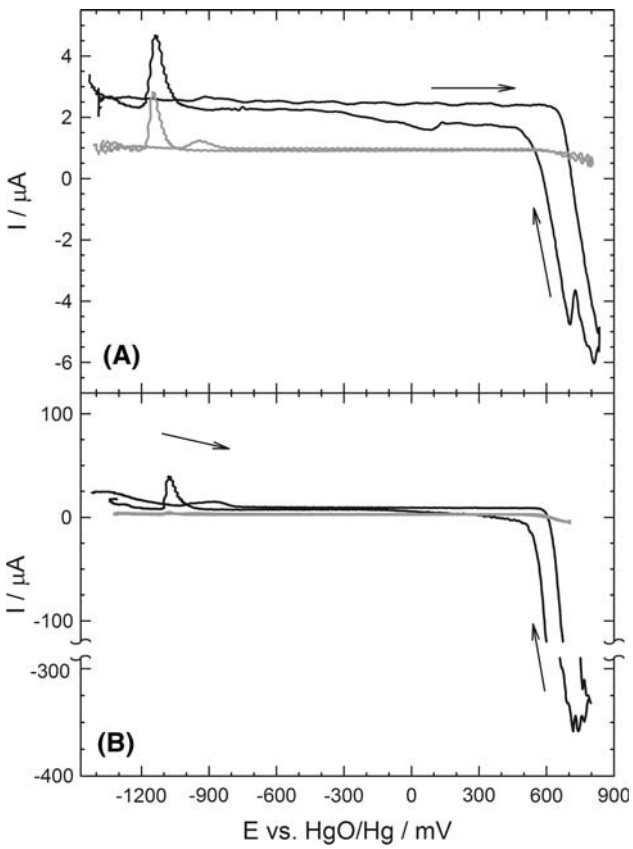

Fig. 2 Comparison of the current response of the Pt-ring electrode held at 300 mV to the processes taking place at the Fe-disk electrode at 20 °C (**a**) and 60 °C (**b**) in NaOH (*black line*) and in KOH (*gray line*) solution. Potential sweep rate of the Fe-disk electrode: 20 mV s^{-1}, electrode rotation rate 1000 rpm

The responses of the Pt-ring electrode kept at a potential of 300 mV, shown in Fig. 2, prove the origin of the individual current peaks [18, 20]. This potential was chosen on the basis of previously published data showing that ferrate(VI) reduction already starts at the Pt electrode at 400 mV [19]. This is in contrast to the Fe electrode where ferrate(VI) reduction was observed at a more cathodic potential. This is caused by the surface of the Fe electrode being partly passivated [18]. In such case ferrate(VI) reduction is thus kinetically controlled.

In NaOH solution, a single anodic current response appears at the disk potential of −1140 mV at 20 °C. This corresponds to the oxidation of Fe(II) produced in the potential region of current peak AI. No response to the current peaks AII and AIII was observed. This indicates that the corresponding reactions are related only to the formation and/or transformation of a solid anodic surface film. The next cathodic current response occurs at the potentials corresponding to current peak AIV. Two explanations for the origin of this response are conceivable: (i) reduction of ferrate(VI) or (ii) reduction of the oxygen that has evolved at the disk electrode. Due to the coincidence with the potential of peak AIV, the first option appears to be the more probable one.

In the case of KOH solution, the origin of the individual peaks is identical and the above discussion applies in this case, too. Compared to the NaOH solution, the main difference is the intensity of the current response.

A comparison of the CV curves obtained in the two electrolytes (Fig. 1) mainly reveals a shift in the potential of the ferrate(VI) reduction in the KOH solution to more cathodic values when compared to NaOH. The minor difference then consists in a change in the significance of the anodic peaks corresponding to active iron dissolution, oxo-hydroxide surface film formation and/or its reduction to the oxidation states Fe(II) and Fe(0). These are more pronounced at 60 °C. The differences in the shape of the polarization curve as such do not indicate marked changes in the reaction mechanism; it rather corresponds to changes in the properties of the layer covering the anode surface. This especially concerns the potential shift in the ferrate(VI) reduction peak CIII. This is explained by a notable inhibition of the electrode surface probably covered by the precipitated iron electrode oxidation products soluble in NaOH. The increased current densities of peaks CI and CII in case of KOH solution should be mentioned as supporting evidence. This is caused by solid intermediates depositing at the electrode surface. These supply the electroactive species during reduction to a greater extent when compared to the NaOH solution where the products and intermediates remain in a homogeneous phase and can easily diffuse

from the electrode surface. By increasing the temperature to 60 °C, the impact of the higher aggressiveness of the environment can be observed and this is documented by generally increased current densities.

Similar conclusions can also be derived from a comparison of Figs. 1 and 2. Here the electric charge corresponding to the current density peak CIII in Fig. 1 is notably higher in the case of KOH, especially at higher temperatures. This indicates a higher amount of ferrate(VI) present at the electrode surface and ready to be reduced in contrast to the NaOH solution. When using an iron-rotating disk electrode, the current response to peak AIV on the platinum-ring electrode was always higher in the case of NaOH. This supports the suggestion that, in the KOH electrolyte, the ferrate(VI) formed precipitates at the electrode surface and it is subsequently incorporated into the layer that has developed there. Only a small portion of the product diffuses into the solution.

As this study focuses largely on the chemistry of electrochemical ferrate(VI) formation, only the part of the polarization curve directly connected with this process will be discussed in more detail in the following text. Fig. 1a and b shows two limiting cases of the development of iron polarization curve in the transpassive region. Whereas at 20 °C, the current shoulder corresponding to ferrate(VI) formation is well defined in all electrolytes; at 60 °C, it is overlapped to a significant degree by the oxygen evolution reaction. The potential when the shoulder begins to rise was determined for all the experimental conditions under study (i.e., electrolyte composition and temperature). The results can be summarized as follows. The potential value decreases with increasing temperature. The average value of this potential decrease is 50 mV for the temperature increase from 20 to 60 °C. Similarly, a potential decrease was observed for the increase of the K^+ content in the electrolyte. A comparison of KOH and NaOH shows for this decrease values 50 and 70 mV for 20 and 60 °C, respectively. This behavior is surprising with respect to the low intermediate and final products potassium salts solubility. An inhibition of the electrode surface expressed by a potential shift in the anodic direction was expected here for K^+-containing electrolytes.

In the case of the pure electrolytes the increasing temperature obviously has a positive effect on the kinetics of the electrode reaction. This is reflected by the commencement of the anodic reaction at the lower electrode potential. Except for the pure NaOH solution, the temperature does not exhibit a strong influence on the Tafel slope of the rise in the current shoulder. In the case of NaOH, it rose from 108 to 120 mV dec^{-1} when the temperature increased from 20 to 60 °C. According to the theory of the kinetics of electrode reactions, these values closely correspond to the number of exchanged electrons $n = 1$ (assuming $\alpha_K = 0.5$). Regarding the obtained Tafel slope values a variation of the electrolyte composition manifests a significant impact. The lowest value of the Tafel slope of 95 mV dec^{-1} was observed for the electrolyte containing Na^+/K^+ in a ratio 1:3. It should be noted that there is no information at the moment on the rate-determining step in the iron anode dissolution and subsequent ferrate(VI)-formation mechanism. The reaction described by Eq. 6 may be considered to be a probable alternative [25].

$$FeOOH + 3OH^- \rightarrow FeO_3^{2-} + 2H_2O + e^- \quad (6)$$

This observation is in agreement with the fact that the oxidation of iron atoms by more than one oxidation degree in a single step is hardly probable. The changes in the Tafel slope observed for the electrolytes with varying Na^+ and K^+ ratios are most probably related to the change in the rate-determining step or in a combination of two or more mechanism steps.

In order to obtain more detailed information on the kinetics of iron anode dissolution and ferrate(VI) formation in dependence on the nature and temperature of the electrolyte used, Koutecky-Levich analysis, Eq. 7, of the current shoulder AIV was performed [26].

$$\frac{1}{j_T} = \frac{1}{j_K} + \frac{1}{j_D} \quad (7)$$

where j_T stands for the experimentally determined current density, j_K for the charge transfer kinetics-limited current density, and j_D for the mass transfer-limited current density. The diffusion part j_D obeys the Levich equation (Eq. 8) and is directly proportional to square root of the rotation rate.

$$j_D = 0.620\, nF\, \pi\, r^2\, D_A^{\frac{2}{3}}\, \upsilon^{-\frac{1}{6}}\, c_A^b\, \omega^{\frac{1}{2}} \quad (8)$$

Here n stands for the number of electrons exchanged, F for the Faraday constant 96485 C mol^{-1}, r for the electrode radius, D_A for the diffusion coefficient of electroactive specie A, υ for kinematic viscosity, c_A^b for the concentration of the electroactive specie A in the bulk of the solution, and ω for the angular rotation rate of the electrode.

The value of the highest current density attainable under conditions of charge transfer kinetics as a rate-determining step can be obtained by extrapolating the j_T^{-1} dependence on $\omega^{-\frac{1}{2}}$ to the infinite electrode rotation rate. The results obtained are summarized in Fig. 3 and Table 1. They document well the significant impact of temperature on the process.

It has already been observed that, at 20 °C the increasing electrode rotation rate results in decreasing current density (with the exception of pure KOH, where current density seems to be independent of rotational speed), at 60 °C the situation is just the opposite. Here the current density increases with increasing rotational speed in all

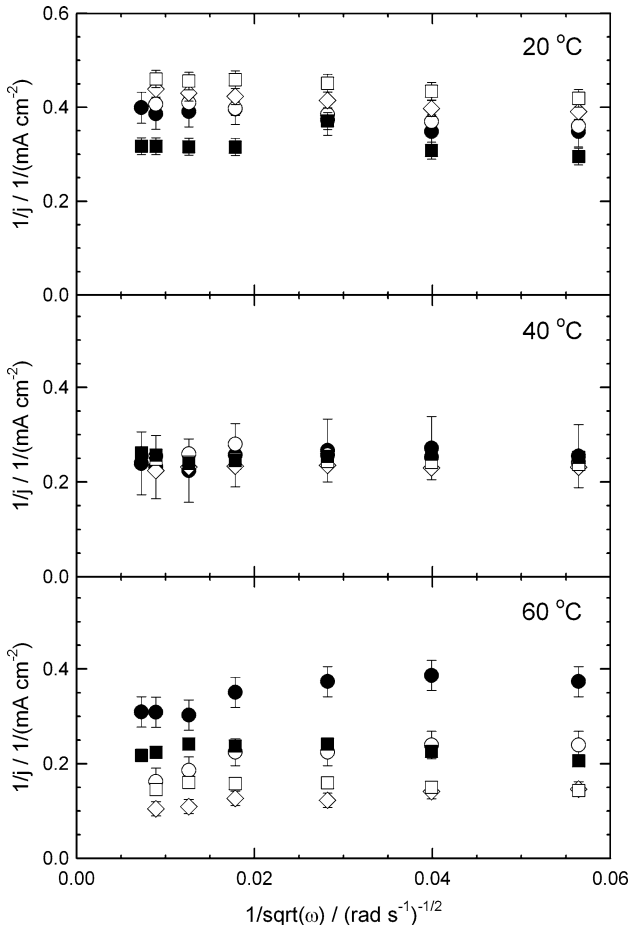

Fig. 3 Dependence of the inverse value of current density of the ferrate(VI)-formation shoulder AIV on the inverse value of the square root of the electrode rotation rate: *filled circle* NaOH, *filled square* KOH, *open circle* Na/K = 3:1, *open diamond* Na/K = 1:1, *open square* Na/K = 1:3. The temperature used is given in the figure

cases (not shown here). This behavior indicates that the reaction mechanism comprises a relatively slow chemical and/or electrochemical step which, at 20 °C, is the rate-determining one. The decrease in current density with increasing rotation rate further confirms the presence of a soluble intermediate in the reaction mechanism. If the K^+ ions are present in the solution, at least part of the intermediate product precipitates at the electrode surface. Thus, contrary to pure NaOH where high solubility of the intermediate results in its removal from the electrode surface, in the case of solutions with higher K^+ content the reaction is not significantly influenced by the electrode rotation rate.

3.2 Electrochemical impedance spectroscopy analysis

EIS was used to quantify the information obtained in the CV and RRDE studies. This technique is capable of providing complementary information on the structure and properties of surface layers. An example of impedance spectra obtained at the potential of 600 mV for the individual solutions under study is shown in Fig. 4a and b for temperatures 20 and 60 °C, respectively.

In agreement with previously published data [27, 28], the system shows two kinetic constants. Thus, an equivalent circuit based on the physical model of two macrohomogeneous surface layers with different properties [27, 28] was used to evaluate the EIS data. Its schematic sketch is shown in Fig. 5.

It consists of two parallel R-CPE elements characterizing individual sublayers connected in series. The last element represents the resistance of the electrolyte. Constant phase element (CPE) was used instead of capacitance to describe the nonideality of the system. The agreement of the model with the experimental data is documented for the temperature of 20 °C in Fig. 4a. The lines represent the results of the model used.

The optimized parameters of the equivalent circuit for the Fe electrode polarized in the pure NaOH solution in dependence on the electrode potential are shown in Fig. 6. The data obtained are in good agreement with the previous results [21]. The resistance element corresponding to the inner, protective oxidic layer shows resistivity two to three orders of magnitude higher when compared to the outer one. In the transpassive potential region it decreases exponentially with increasing electrode potential. Moreover, the temperature causes an exponential decrease in resistivity values at the given electrode potential. The capacity of the outer layer increases with increasing potential by almost two orders of magnitude. After exceeding a certain potential limit the capacity starts to decrease again. Such behavior corresponds either to the decreasing thickness of the outer sublayer or to an increase in its specific surface, followed at high anodic potentials by its disintegration. Additional information is needed to

Table 1 The values of the kinetic current density (mA cm^{-2}) obtained with the Fe electrode in the potential region of peak AIV at the studied temperatures in 14-M OH^- solutions with various Na^+/K^+ ratios

Solutions		NaOH	Na^+/K^+ = 3:1	Na^+/K^+ = 1:1	Na^+/K^+ = 1:3	KOH
j_K	20 °C	1.95 ± 0.03	2.39 ± 0.02	2.26 ± 0.02	2.12 ± 0.02	2.53 ± 0.02
	40 °C	4.23 ± 0.07	3.71 ± 0.01	4.357 ± 0.004	4.027 ± 0.004	3.968 ± 0.006
	60 °C	8.48 ± 0.03	5.75 ± 0.03	9.81 ± 0.02	6.313 ± 0.007	5.081 ± 0.005

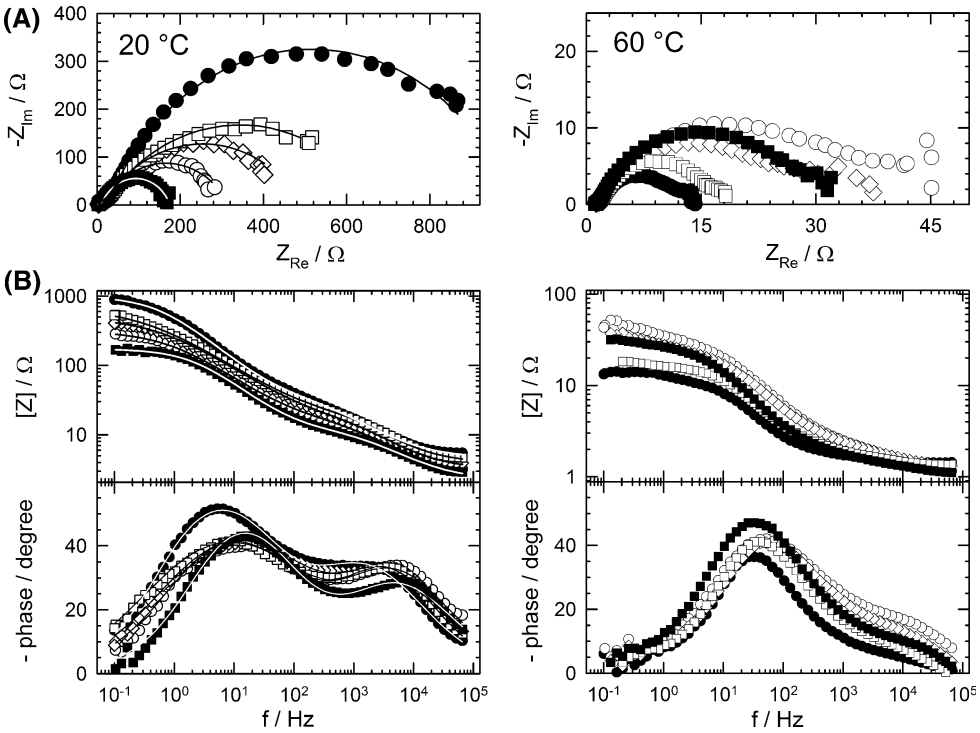

Fig. 4 Nyquist and Bode plots of impedance spectra of pure Fe electrode at 600 mV at 20 °C (on the *left*) and 60 °C (on the *right*) obtained in the electrolytes studied: *filled circle* NaOH, *filled square* KOH, *open circle* Na/K = 3:1, *open diamond* Na/K = 1:1, *open square* Na/K = 1:3. The *lines* denote the results of the optimized equivalent circuit given in Fig. 5

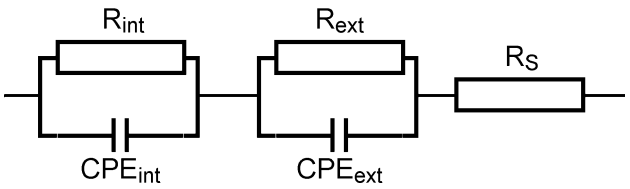

Fig. 5 Equivalent circuit proposed for the evaluation of experimental data. R_S—electrolyte resistance; index *ext* denotes the external sublayer, index *int* the internal sublayer

establish the true mechanism. The inner layer is more stable as its capacity only increases slowly with polarizing potential. An increasing dependence of layer capacity on increasing temperature is well detectable for both sublayers. In the case of the inner sublayer, however, more aggressive conditions are needed to induce related changes. It does not start until high anodic potentials and/or a high temperature are applied.

The additional information needed is provided by the values of the CPE parameter ϕ shown in Fig. 6c. The significant decrease of the ϕ values with the potential for the outer layer indicates changes in the sublayer structure. This can be assigned to its specific surface increase. It means that the increase of layer capacity with increasing potential discussed above is more probably related to the gradual destruction of the layer than to its reduction in thickness. That is also the reason for its decrease in resistivity. In the case of the inner sublayer, the development of this parameter value indicates a gradual change in the surface to a more regular one. Thus, in this case, the observed changes in capacity more probably correspond to the gradual reduction of its thickness. This is in agreement with the higher stability of this sublayer stated previously. The temperature shows only a minor impact on the parameter ϕ value. It can thus be concluded that temperature has significant impact on the thickness of both the sublayers, but not on their structure. This is in agreement with the theory concerning the mechanism of its influence on the surface behavior of the anode consisting in a chemical interaction of the OH^- anion with surface layers.

The dependence of the inner layer's resistivity on the content of the K^+ ion in the mixture is illustrated in Fig. 7 (on the left). It is shown for the electrode potentials of 600 mV at a temperature of 20 °C, 575 mV at 40 °C, and 550 mV at 60 °C. These potentials were chosen because they fall into the potential range of intensive ferrate(VI) formation and not yet well-developed oxygen evolution.

The situation is clear at 20 °C. The resistivity of the two sublayers monotonously decreases with increasing K^+ content. At 40 °C, the maximum resistivity of the inner layer appears at Na^+/K^+ content equal to 1:3. The main difference to the lower temperature consists in a significant decrease of the resistivity values observed for the solutions with a high Na^+ content. In the case of 60 °C, the highest resistance was observed for the mixed Na^+/K^+ solution with a ratio of 3:1. Otherwise no clear dependence on the solution composition was identified.

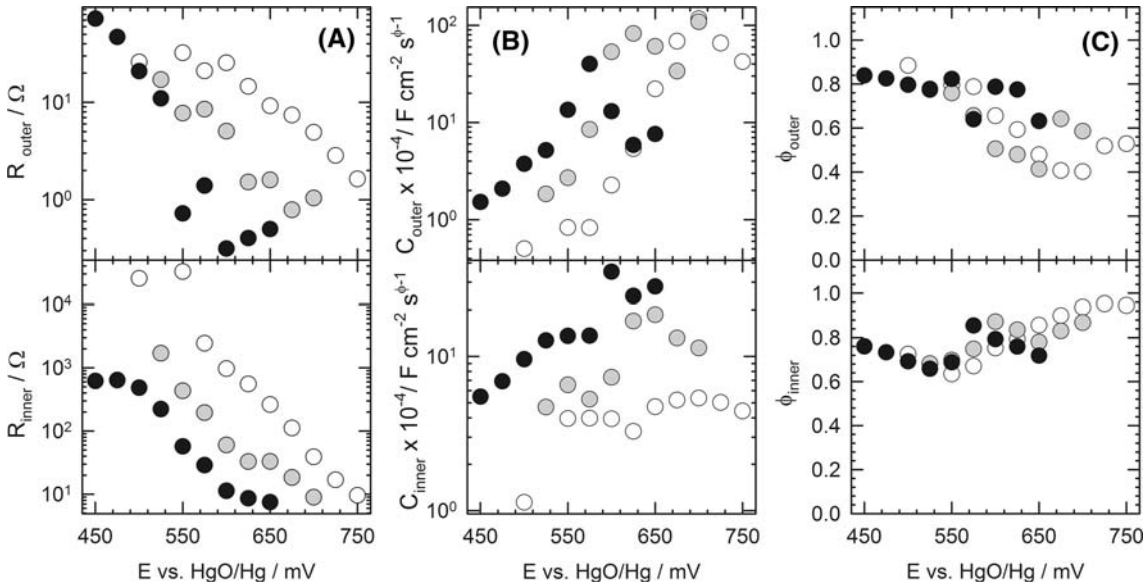

Fig. 6 The fitted values of the equivalent circuit elements: resistance (**a**), capacitance (**b**), and parameter ϕ (**c**) obtained for the layers in dependence on the anodic polarization potential of the Fe electrode in pure NaOH electrolyte for various temperatures: 20 °C *white*, 40 °C *gray*, and 60 °C *black* symbols

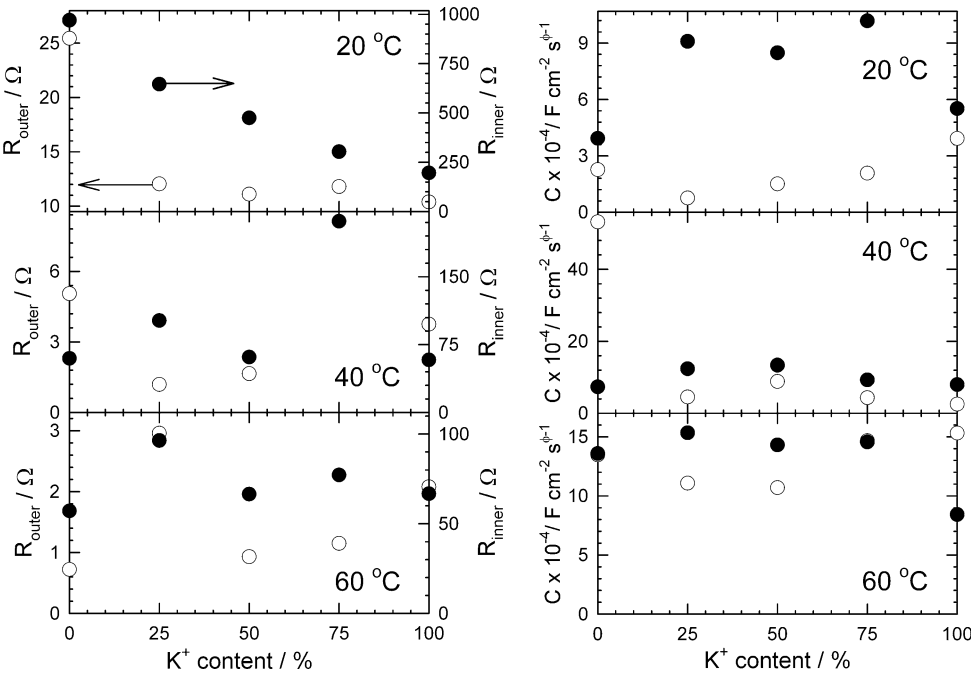

Fig. 7 The fitted values of resistances (*left*) and capacitances (*right*) obtained for the outer (*open circle*) and inner (*filled circle*) layers at a potential of 600 mV at 20 °C, 575 mV at 40 °C, and 550 mV at 60 °C in dependence on electrolyte composition, i.e., K^+ ion content in the 14-M OH^- solution

In the case of the capacitance of the individual layers, in Fig. 7 (on the right) it is possible to see that both of them show a significant dependence on the K^+ content in the anolyte. Whereas the capacitance of the internal sublayer is increased using a mixture of the two cations, in the case of the external sublayer the situation is just the opposite. The system with pure KOH electrolyte shows interestingly lower value of internal sublayer resistivity as well as capacity than for the NaOH–KOH mixtures in the entire temperature range. This indicates that the anode behavior observed is not just a consequence of the intermediate or final product's precipitation on the anode surface. Different kinetic aspects have to be considered as well. The present results do not provide sufficient information to explain this behavior.

Whereas the effects of temperature or applied potential could be specified easily, in the case of the K^+ cation addition the situation was not so clear. Neither

potentiodynamic methods nor impedance measurements provided completely clear information. Therefore, galvanostatic batch electrolyses were performed to provide additional independent information.

3.3 Batch electrolysis results

The efficiency of iron electrode anodic dissolution was calculated with respect to ferrate(VI) formation and its dependence on the applied current density is shown in Fig. 8 for all electrolytes studied. The effect of temperature together with the electrolyte composition is especially significant in the case of pure electrolytes. Whereas in the case of KOH the efficiency of electrolysis gradually increases with increasing temperature, in the case of NaOH the temperature of 40 °C corresponds to the optimal performance. This is in agreement with previously published results [12, 17]. At lower temperatures, the solution does not provide sufficiently aggressive conditions for effective activation of the anode surface. At higher temperatures, the rapid decomposition of ferrate(VI), formed in the homogeneous phase, back to Fe^{III+} proceeds. In the case of KOH, a solid ferrate(VI) which is less sensitive to decomposition under the conditions applied is formed directly at the electrode surface. This is documented in Fig. 9, where dependences of $c_{(Fe_{tot})} - c_{(FeO_4^{2-})}$, corresponding to the results given in Fig. 8, are plotted.

The effect of an addition of the second cation K^+ to the solution is notable at all temperatures under study. At 20 and 40 °C, even a 3.5-M addition of K^+ leads to a significant drop in the current efficiency of the process. By contrast, at 60 °C, this addition results in more efficient ferrate(VI) production when compared to the pure NaOH solution. The optimum performance was observed for the solution containing Na^+/K^+ in a ratio of 3:1 at this temperature. Similar dependencies were also obtained by Lapicque and Valentin [16] even though they studied different anode material. By comparing Figs. 8 and 9, it was noticed that the decomposition of ferrate(VI) in electrolysis is relatively low for all solutions with added K^+ ion. This is a consequence of a

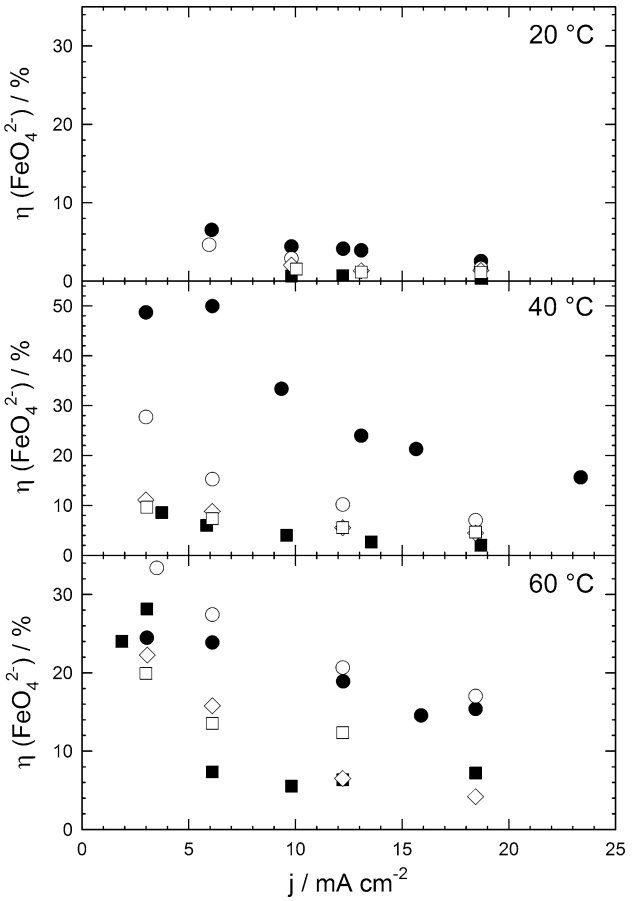

Fig. 8 Dependence of current efficiency of ferrate(VI) formation after 180 min of batch electrolysis on anodic current density at various temperatures obtained for the individual electrolytes used: *filled circle* NaOH, *filled square* KOH, *open circle* Na/K = 3:1, *open diamond* Na/K = 1:1, *open square* Na/K = 1:3

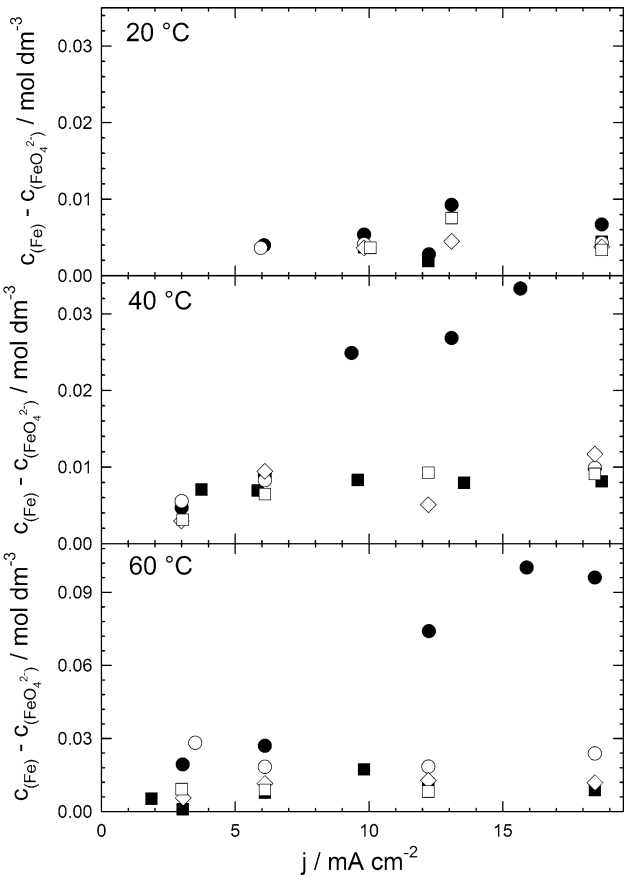

Fig. 9 Dependence of the difference in molar concentration of the total iron and FeO_4^{2-} contained in the electrolyte after finishing the electrolysis on the anodic current density applied at various temperatures for the individual electrolytes under study: *filled circle* NaOH, *filled square* KOH, *open circle* Na/K = 3:1, *open diamond* Na/K = 1:1, *open square* Na/K = 1:3

significant decrease in solubility of the ferrate(VI) product caused by the change in electrolyte composition. This results in a significant stabilization of the product.

4 Conclusions

The electrolyte composition was proven to have an important impact on iron electrode behavior during electrochemical ferrate(VI) synthesis. This was established by cyclic voltammetry as well as by EIS. The results were finally supported by batch electrolysis experiments. Whereas in the low temperature range the highest synthesis current efficiency of 6.5 and 50.0%, for 20 and 40 °C, respectively, was attained using a pure NaOH electrolyte at the highest temperature applied, i.e., 60 °C, the highest current efficiency of 33.4% was obtained for the mixed electrolyte containing Na^+/K^+ in a ratio of 3:1. Comparable results were also achieved with the other solutions with added K^+ ion, especially at low current densities. In the case of temperatures of 20 and 60 °C, the solutions indicating the highest resistivity of the internal as well as the external sublayer to the charge transfer show optimal behavior in terms of the current efficiency of the process with respect to ferrate(VI) formation. At 40 °C, this corresponded to the second highest efficiency observed. This was explained in terms of decelerating oxygen evolution as a parasitic anode reaction promoted by increasing anodic charge transfer kinetics. The positive influence of the K^+ ion addition to the anolyte at elevated electrolysis temperature consists in the suppression of the oxygen evolution reaction and at the same time in the stabilization of the product by its precipitation in the solid form.

Acknowledgments The financial support of this study by the Ministry of Education, Youth and Sports of the Czech Republic under Project No.: ME890 and CEZ: MSM6046137301 is gratefully acknowledged. V. K. Sharma acknowledges support of N.S.F. (CHE 0706834).

References

1. Mellor JW (1924) A comprehensive treatise on inorganic and theoretical chemistry. Longmans, Green & Co, London
2. Macova Z, Bouzek K, Hives J et al (2009) Electrochim Acta 54:2673
3. Eisen in Gmelins Handbuch No. 59 (1932)
4. Hrostowski HJ, Scott AB (1950) J Chem Phys 18:105
5. Thompson GW, Ockerman LT, Schreyer JM (1951) J Am Chem Soc 73:1379
6. Poggendorf JC (1841) Pogg Ann 54:372
7. Haber F (1900) Z Elektrochem 7:215
8. Pick W (1901) Z Elektrochem 7:713
9. Toušek J (1962) Coll Czech Chem Commun 27:914
10. Bouzek K, Roušar I (1996) J Appl Electrochem 26:919
11. Bouzek K, Roušar I, Taylor MA (1996) J Appl Electrochem 26:925
12. Bouzek K, Roušar I (1997) J Appl Electrochem 27:679
13. Denvir A, Pletcher D (1996) J Appl Electrochem 26:815
14. Bouzek K, Schmidt MJ, Wragg AA (1999) Electrochem Commun 1:370
15. Bailie GA, Bouzek K, Lukášek P et al (1996) J Chem Technol Biotechnol 66:35
16. Lapicque F, Valentin G (2002) Electrochem Commun 4:764
17. He W, Wang J, Shao H et al (2005) Electrochem Commun 7:607
18. Beck F, Kaus R, Oberst M (1985) Electrochim Acta 30:173
19. Bouzek K, Roušar I, Bergmann H et al (1997) J Electroanal Chem 425:125
20. Venkatadri AS, Wagner WF, Bauer HH (1971) Anal Chem 43:1115
21. Bouzek K, Bergmann H (1999) Corros Sci 41:2113
22. De Koninck M, Bélanger D (2003) Electrochim Acta 48:1435
23. Zou J-Y, Chin D-T (1988) Electrochim Acta 33:477
24. Denvir A, Pletcher D (1996) J Appl Electrochem 26:823
25. Bouzek K, Roušar I (1993) J Appl Electrochem 23:1317
26. Treimer S, Tang A, Johnson DC (2002) Electroanal 14:165
27. Híveš J, Mácová Z, Benová M et al (2008) J Electrochem Soc 155:E113
28. Híveš J, Benová M, Bouzek K et al (2008) Electrochim Acta 54:203